Artefact calibration of parallel mechanism, kinematic calibration with *a priori* knowledge

**Osamu Sato[1], Ken Shimojima[2], Ryoshu Furutani[2]
and Kiyoshi Takamasu[1]**

[1] The University of Tokyo, 7-3-1 Hongo, Bunkyo, Tokyo 113-8656, Japan
[2] Tokyo Denki University, 2-2 Kanda-Nishiki Cho, Chiyoda, Tokyo 101-0057, Japan

E-mail: ri@nano.pe.u-tokyo.ac.jp (O Sato)

Abstract
In the application of parallel mechanisms, it is necessary to calibrate the kinematic parameters and improve the positioning accuracy for accurate task performance. However, there are strong correlations between all the parameters in the kinematic calibration of a parallel mechanism. Therefore, it is difficult to identify all kinematic parameters included in a kinematic model of the parallel mechanism from measuring data. In this study, we proposed to use *a priori* knowledge of the kinematic parameters to eliminate their correlation and to give robustness to the calibration. *A priori* knowledge can be given without extra measurement when the manufacturing process of the mechanism is under quality control. Using *a priori* knowledge, all kinematic parameters of the parallel mechanism are identified in the *artefact calibration* without divergence. First, an *artefact calibration* with *a priori* knowledge is formulated. Second, the estimation of *a priori* knowledge under quality control is described. Finally, the robustness and effectiveness of the *artefact calibration* with *a priori* knowledge is demonstrated through simulations.

Keywords: parallel mechanism, geometric calibration, kinematic calibration, artefact calibration, *a priori* knowledge, least squares method

1. Introduction

To improve a robot's accuracy, it is necessary to improve both its repeatability and accuracy of positioning. In the case of a parallel mechanism, the improvement of accuracy is difficult in contrast to the improvement of repeatability because of the difficulty in the calibration, in which all kinematic parameters whose error results in a non-negligible positioning error of the end-effector must be identified [1, 2]. However, parameter identification for a parallel mechanism is challenging, because there are strong correlations among all the parameters. The correlations are derived from closed kinematic chains composed in the calibration system [3]. To calibrate a parallel mechanism, we must eliminate these correlations. One method for eliminating correlations is to change the arrangement of the measurement of the end-effector location [4]. Another is to change the observation equation in the least squares method [5]. However, these methods are not enough to give robustness to the calibration.

In this study, we propose to use *a priori* knowledge of the kinematic parameters to eliminate correlations. Usually, *a priori* knowledge of each parameter is given through its direct measurement. Hence, extra measurements are needed. Moreover, *a priori* knowledge is difficult to obtain when direct measurement is hard or impossible. Here we assume that the manufacturing process of the mechanism is under quality control, each true value of a kinematic parameter is close to its design value and the parameter's error is within
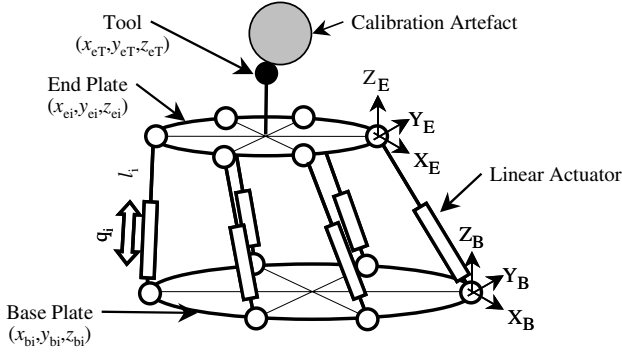
Figure 1. Calibration model of a Stewart Platform.

the design tolerance, which means we can use the design value and its tolerance for *a priori* knowledge. In this case, no extra measurement is needed and *a priori* knowledge of any parameter is available. Using *a priori* knowledge, all kinematic parameters of the parallel mechanism are identified in the kinematic calibration using calibration artefacts (*artefact calibration*) with the least squares method.

First, *artefact calibration* with *a priori* knowledge is formulated. Second, the estimation of *a priori* knowledge of all kinematic parameters from their design values and tolerances is described. Finally, the *artefact calibration* for the parallel mechanism with *a priori* knowledge is demonstrated. Using this method, all kinematic parameters are converged to adequate values.

2. Formulation

Figure 1 shows a calibration system of a six degrees of freedom Stewart Platform. The main components of the Stewart Platform are a hexagonal base plate, six linear actuators with encoders and a hexagonal end plate. The components are connected with spherical joints, and a tool is fixed on the end plate. To calibrate the Stewart Platform, some calibration artefacts, for example, the block gauge, ring gauge, double ball bar and so on, are arranged in its workspace and, through their measurement, the kinematic parameters included in kinematic models of the Stewart Platform are identified.

2.1. Kinematic parameters

To improve a robot's accuracy through calibration, true values of all kinematic parameters whose variations lead to large geometrical pose errors of the robot should be approximated. The first step of *artefact calibration* is describing the kinematic model of the mechanism with necessary and sufficient kinematic parameters [6]. A classical modelling method for robots is to use the Danavit–Hartenberg parameters [7], but this method is not effective for describing the calibration model [8]. Here, we describe the calibration model only with linearly independent parameters [8–10].

Two coordinate systems are set up for the Stewart Platform. The fixed coordinate system $B\{X_B, Y_B, Z_B\}$ is located at the centre of a spherical joint on the base plate. The mobile coordinate system $E\{X_E, Y_E, Z_E\}$ is located at the centre of a spherical joint on the end plate [9, 10].

2.1.1. Base plate. The base plate is described as a rigid polyhedron whose vertices are at the positions of each spherical joint in the fixed coordinate system. Thus, we describe the base plate with 18 parameters ($x_{b1}, y_{b1}, z_{b1}, \ldots,$ x_{b6}, y_{b6}, z_{b6}). Six of these 18 parameters should be checked off the parameter identification objects because they are linearly dependent on the others. Therefore we consider these six parameters, $x_{b1}, y_{b1}, z_{b1}, x_{b2}, z_{b2}, z_{b3}$, as constants.

2.1.2. Linear actuator. Linear actuators are described as segments whose lengths are the sum of the initial length plus each expansion. Expansion can be measured with the encoder attached to it. However, the initial lengths of the linear actuators are unknown. Hence we introduce six parameters for these initial lengths ($l_1, l_2, \ldots, l_6$).

2.1.3. End plate and tool. The end plate is described as a rigid polyhedron whose vertices are at the positions of each spherical joint in the mobile coordinate system. Thus, we describe the end plate with 18 parameters ($x_{e1}, y_{e1}, z_{e1}, \ldots, x_{e6}, y_{e6}, z_{e6}$). The tool is also described as a vertex of the polyhedron in the same coordinate system. Hence it is described with three parameters (x_{eT}, y_{eT}, z_{eT}). As in the case of the base plate, six parameters of these 21 parameters should be checked off the parameter identification objects. Therefore we consider these six parameters, $x_{e1}, y_{e1}, z_{e1}, x_{e2}, z_{e2}, z_{e3}$, as constants.

2.1.4. Calibration artefact. In this paper, we use balls whose radii are known for calibration artefacts. We arrange n balls in the workspace of a Stewart Platform. In this case, it is necessary to identify the position of the centre of each ball in the fixed coordinate system. Therefore, we introduce $3 \times n$ parameters for these centres ($x_{c1}, y_{c1}, z_{c1}, \ldots, x_{cn}, y_{cn}, z_{cn}$).

2.2. Calibration formulation

Kinematics of the Stewart Platform are described as follows [11]:

$$|\boldsymbol{B}_i - A_{E\rightarrow B}\boldsymbol{E}_i| = l_i + q_i, \qquad (i = 1, \ldots, 6), \qquad (1)$$

where $\boldsymbol{B}_i$ are the coordinates of the ith spherical joint $(x_{bi}\ y_{bi}\ z_{bi})^T$ in the coordinate system on the base plate, $\boldsymbol{E}_i$ are the coordinates of the ith spherical joint $(x_{ei}\ y_{ei}\ z_{ei})^T$ in the coordinate system on the end plate, l_i and q_i are the initial length and expansion, respectively, of the ith linear actuator which connects the ith joint on the base plate and the ith joint on the end plate and $A_{E\rightarrow B}$ is the coordinate transformation from the coordinate system on the end plate to that on the base plate. Solving equation (1) for $A_{E\rightarrow B}$, the forward kinematic solution $\boldsymbol{f}$, the position of the end of the tool in the fixed coordinate system, is given by

$$\boldsymbol{f}(\boldsymbol{q}, \boldsymbol{p}) = A_{E\rightarrow B}\boldsymbol{E}_T, \qquad (2)$$

where $\boldsymbol{q}$ is the expansion vector of linear actuators when the tool is positioned on the surface of a calibration ball and $\boldsymbol{p}$ is the kinematic parameter vector as follows:

$$\boldsymbol{p} = (y_{b2} \quad \ldots \quad z_{b6} \quad l_1 \quad \ldots \quad l_6 \quad y_{e2} \quad \ldots \quad z_{eT})^T. \quad (3)$$

1159

When we position the tool on a ball m times, the observation equations vector is given by

$$O = \begin{bmatrix} c(f(q_{11}, p)) \\ \vdots \\ c(f(q_{ij}, p)) \\ \vdots \\ c(f(q_{nm}, p)) \end{bmatrix}, \quad (4)$$

where c is the function vector of the forward kinematic solution $f(q, p)$ and q_{ij} is the expansion vector of the linear actuators at the jth position on the ith ball.

The kinematic parameter vector is calculated as the least squares solution by the Newton–Raphson method as follows:

$$p_{\text{new}} = p_{\text{old}} + (J^T W^{-1} J)^{-1} J^T W^{-1} O, \quad (5)$$

where W is the error matrix associated with the measurement, and the Jacobian matrix J is

$$J = \begin{bmatrix} \partial c(f(q_{11}, p))/\partial p_1 & \cdots & \partial c(f(q_{11}, p))/\partial p_k \\ \vdots & \ddots & \vdots \\ \partial c(f(q_{nm}, p))/\partial p_1 & \cdots & \partial c(f(q_{nm}, p))/\partial p_k \end{bmatrix}. \quad (6)$$

2.3. Parameter identification with a priori knowledge

When we calibrate kinematic parameters p from the same measurement data set $\{q\}$, we can obtain better solutions by choosing an adequate formulation of the observation equation that presents a good calculation condition of the least squares method. Furthermore, we can make a robust calibration under difficult conditions when *a priori* knowledge of each parameter is available.

Using *a priori* knowledge, equations (4) and (6) are reconfigured as follows:

$$\hat{O} = \begin{bmatrix} c^T \mid p - \acute{p} \end{bmatrix}^T,$$

$$\hat{J} = \begin{bmatrix} J \\ \hline E_{k,k} \end{bmatrix},$$

$$\hat{W} = \begin{bmatrix} W & & O \\ \hline & \sigma_{p_1}^2 & \\ O & & \ddots \\ & & & \sigma_{p_k}^2 \end{bmatrix}, \quad (7)$$

where $\acute{p}$ is *a priori* values of the kinematic parameters estimated from their design specification or some other measurements, $E_{k,k}$ is a $k \times k$ unit matrix and σ_{p_i} is the *a priori* standard deviation of the kinematic parameter p_i which approximates its tolerances. Identified values of p_i are bound around $\acute{p} + o(\sigma_{p_i})$. A reasonable σ_{p_i} provides the robustness for the least squares method, and thus kinematic parameters are identified without divergence.

3. Calibration simulation

We identify kinematic parameters through the measurement of balls whose radii are calibrated. In this section, we compare the results of four simulations using the same measurement data.

Table 1. Conditions of the calibration simulation.

Number of artefacts (balls)	27
Number of measurement point on an artefact	7
Size of artefact (ball)	5 mm (radius)
Error of artefact size	1 μm
Repeatability of linear actuator	1 μm
Repeatability of positioning tool	1 μm

Table 2. Kinematic parameters: design values (upper) and true values (lower) for simulation.

	Base plate (mm)					
x_{b1}	99.620	y_{b1}	−8.716	z_{b1}	0.000
	99.700		−8.633		0.079
x_{b2}	99.620	y_{b2}	8.716	z_{b2}	0.000
	99.604		8.619		−0.078
x_{b3}	−42.262	y_{b3}	90.631	z_{b3}	0.000
	−42.154		90.721		−0.041
x_{b4}	−57.358	y_{b4}	81.915	z_{b4}	0.000
	−57.499		81.730		0.053
x_{b5}	−57.358	y_{b5}	−81.915	z_{b5}	0.000
	−57.449		−81.824		−0.045
x_{b6}	−42.262	y_{b6}	−90.631	z_{b6}	0.000
	−42.202		−90.613		0.033
	Linear actuator (mm)					
l_1	235.000	l_2	235.000	l_3	235.000
	234.934		235.046		235.124
l_4	235.000	l_5	235.000	l_6	235.000
	235.003		235.069		234.931
	End plate (mm)					
x_{e1}	28.679	y_{e1}	−40.958	z_{e1}	0.000
	28.695		−41.025		0.054
x_{e2}	28.679	y_{e2}	40.958	z_{e2}	0.000
	28.766		41.007		0.036
x_{e3}	21.131	y_{e3}	45.315	z_{e3}	0.000
	21.056		45.307		−0.033
x_{e4}	−49.810	y_{e4}	4.358	z_{e4}	0.000
	−49.854		4.441		−0.089
x_{e5}	−49.810	y_{e5}	−4.358	z_{e5}	0.000
	−49.817		−4.418		0.099
x_{e6}	−21.131	y_{e6}	−45.135	z_{e6}	0.000
	21.155		−45.311		−0.067
	Tool (mm)					
x_{eT}	0.000	y_{eT}	0.000	z_{eT}	60.000
	0.099		0.053		60.411

For calibration simulation, we used 27 balls, with 7 calibration points on a ball, for a total of 189 measurement points. The calibration points are chosen at random on the lower hemisphere of each ball. The poses of the tool are also set at random. Then the measurement simulation data q_{ij} are calculated as the inverse kinematic solutions with the given calibration points, poses and the true kinematic parameter values. Other conditions of the simulation appear in table 1. Design values and true values of kinematic parameters appear in table 2. Here we assumed that the *a priori* deviation σ_p is 0.1 mm. The overview of the calibration system is shown in figure 2.

Prior to the calibration, we estimated the positioning accuracy of the Stewart Platform from the law of error propagation with the design values of kinematic parameters and *a priori* covariance matrix

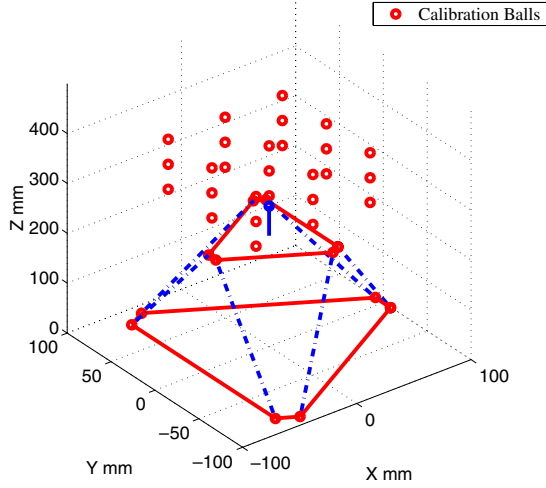$$\Sigma_p = \sigma_p^2 E, \quad (8)$$

Figure 2. Geometric model of the calibration system: Stewart Platform (calibration object) and arrangement of calibration balls (artefacts for calibration).
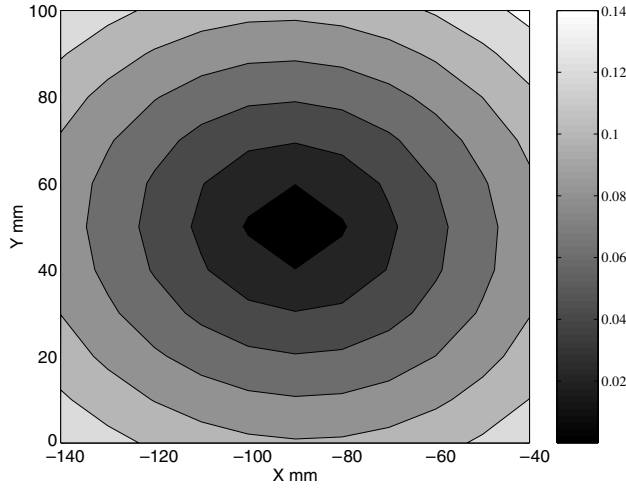

Figure 3. Positioning accuracy of the parallel mechanism before calibration. Positioning accuracy is estimated from the law of error propagation using *a priori* parameter variance σ_p^2 from the design values.

where we assume that there is no correlation between the parameters [12]. Figure 3 shows the standard deviation of positioning accuracy on the horizontal plane $Z = 400$ mm. Positioning accuracy before calibration approximates 0.1 mm.

3.1. Calibration without a priori knowledge

First, we estimate the kinematic parameters without *a priori* knowledge. We made two simulations with different observation equations to observe the effect of changing the observation equation in the calibration.

*3.1.1. Simulation **I**: using the calibrated radii of balls.* Simulation **I** is the parameter identification using the observation equation

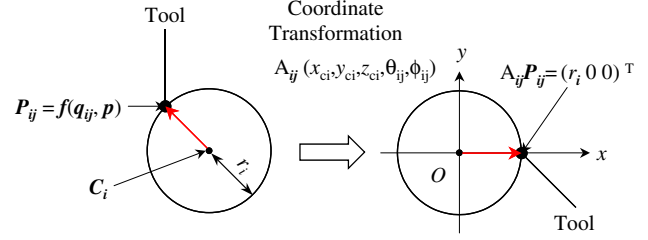$$c_{ij} = r_i - |f(q_{ij}, \hat{p})|, \tag{9}$$

Figure 4. Coordinate transformation using attached extra parameters. The measuring position is transformed to the coordinates $(r_i, 0, 0)$.

where r_i is the calibrated radius of the ith ball and $\hat{p}$ is the vector of parameter identification objects. Equation (9) means that the distance between the centre of the ith ball and the measurement point on it should be equal to the calibrated radius of it. In this calibration, the parameter identification objects are the 33 kinematic parameters shown in table 2 and 81 coordinates of the centres of the balls. Initial values of kinematic parameters are substituted for design values in table 2. Initial coordinates of each ball centre are approximated on the basis of the values derived from the measurement data set $\{q\}$ with the initial kinematic parameters.

Through simulation **I**, identified values of kinematic parameters diverge from their true values. The residual norms of the observation equation vector $|O|$ transits are shown in figure 5. We see from figure 5 that the observation equation written in equation (9) results in a bad calibration condition.

*3.1.2. Simulation **II**: using the transformed coordinates.* Next, we change the observation equation by attaching extra parameters to improve the mathematical condition of the least squares calculation. When we measured the jth position on the ith ball, two extra parameters, θ_{ij}, ϕ_{ij}, were attached to the parameter identification objects. Then, using five parameters, x_{ci}, y_{ci}, z_{ci} and attached θ_{ij}, ϕ_{ij}, the measurement ball and the measured position are transformed as shown in figure 4 [13]. In the new coordinate system, the centre of the ith ball is at the origin of the system and the jth measured position is on the x-axis.

The measured position after transformation should have coordinates $(r_i, 0, 0)$, so we can use the observation equation

$$c_{ij} = \begin{pmatrix} r_i \\ 0 \\ 0 \end{pmatrix} - f(q_{ij}, \hat{p}), \tag{10}$$

where r_i is the calibrated radius of the ith ball and $\hat{p}$ is the vector of parameter identification objects. In this calibration, the parameter identification objects are the 33 kinematic parameters shown in table 2, 81 coordinates of the centres of the balls and 378 coordinate transformation parameters at each measuring position. Initial values of the kinematic parameters and the coordinates of each ball centre are the same as in simulation **I**. Those of the coordinate transformation parameters are calculated from the coordinates of the initial centre of each ball and those of the measuring position calculated from the initial kinematic parameters.

As in simulation **I**, the identified values of kinematic parameters in simulation **II** diverge from their true values. The residual norms of the observation equation vector $|O|$
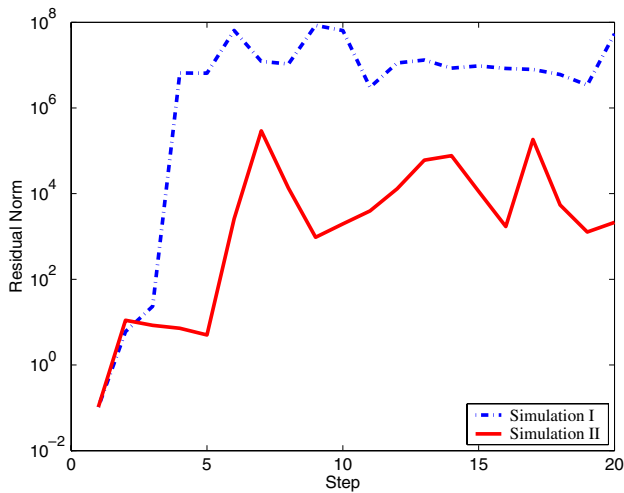
Figure 5. Residual norm at each step in simulations **I** and **II**.

transits are shown in figure 5. We see from figure 5 that it is not enough to change the observation equation to improve the mathematical condition of the simulation.

3.2. Calibration with a priori knowledge

Next, we estimated the kinematic parameters by attaching *a priori* knowledge to simulations **I** and **II**. Through the simulations, we see the effect of *a priori* knowledge on the calibration. At the same time, we see the effect of changing the observation equation again.

*3.2.1. Simulation **III**: using the calibrated radii of balls.* In simulation **III**, we attach *a priori* knowledge to simulation **I**. *A priori* values and standard deviations of kinematic parameters are given in table 2. In this case, the *a priori* standard deviation of each kinematic parameter is approximated to be at most 0.1 mm. Those of the coordinates of each ball centre are given from the initial centre of the ball and the prior error estimation shown in figure 3. In this case, the *a priori* standard deviation of the initial centre is approximated to be at most 0.1 mm.

Through simulation **III**, all kinematic parameters and each ball centre are identified without divergence. The residual norms of the observation equation vector $|O|$ transits are shown in figure 8. We see from figure 8 that *a priori* knowledge gives robustness to the calibration.

Identified values and standard deviations appear in table 3. The overview of the identified calibration system is shown in figure 6. Positioning accuracy after simulation **III** is estimated from the law of error propagation with the identified values of kinematic parameters and covariance matrix. Figure 7 shows the standard deviation of positioning accuracy on the horizontal plane $Z = 400$ mm. Positioning accuracy improved from 0.1 mm to 80 μm through simulation **III**.

*3.2.2. Simulation **IV**: using the transformed coordinates.* In simulation **IV**, we attach *a priori* knowledge to simulation **II**. *A priori* values and standard deviations of the kinematic
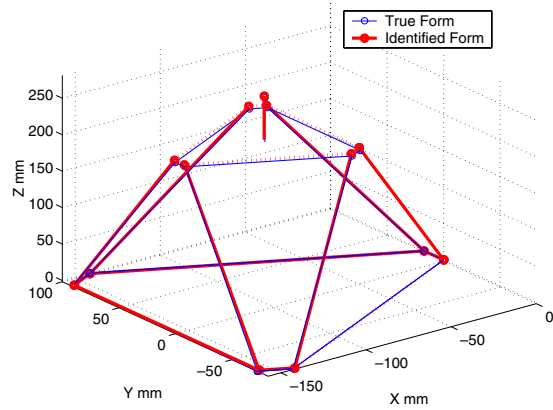

Figure 6. Identified form of the parallel mechanism (simulation **III**). (This figure is in colour only in the electronic version)

Table 3. Results of simulation **III**: identified values (upper) and standard deviations (lower).

	Base plate (mm)				
x_{b1}	0 (nominal)	y_{b1}	0 (nominal)	z_{b1}	0 (nominal)
	0 (nominal)		0 (nominal)		0 (nominal)
x_{b2}	0 (nominal)	y_{b2}	17.362	z_{b2}	0 (nominal)
	0 (nominal)		0.087		0 (nominal)
x_{b3}	−141.7968	y_{b3}	99.3614	z_{b3}	0 (nominal)
	0.078		0.086		0 (nominal)
x_{b4}	−156.955	y_{b4}	90.609	z_{b4}	−0.078
	0.087		0.083		0.088
x_{b5}	−156.967	y_{b5}	−73.178	z_{b5}	−0.045
	0.087		0.083		0.088
x_{b6}	−141.884	y_{b6}	−81.982	z_{b6}	0.080
	0.079		0.082		0.087
	Linear actuator (mm)				
l_1	235.041	l_2	234.972	l_3	235.101
	0.076		0.071		0.074
l_4	234.972	l_5	234.960	l_6	235.069
	0.082		0.083		0.082
	End plate (mm)				
x_{e1}	0 (nominal)	y_{e1}	0 (nominal)	z_{e1}	0 (nominal)
	0 (nominal)		0 (nominal)		0 (nominal)
x_{e2}	0 (nominal)	y_{e2}	81.927	z_{e2}	0 (nominal)
	0 (nominal)		0.085		0 (nominal)
x_{e3}	−7.654	y_{e3}	86.332	z_{e3}	0 (nominal)
	0.074		0.083		0 (nominal)
x_{e4}	−78.490	y_{e4}	45.444	z_{e4}	0.044
	0.077		0.081		0.088
x_{e5}	−78.487	y_{e5}	36.474	z_{e5}	0.132
	0.080		0.079		0.087
x_{e6}	−7.532	y_{e6}	−4.331	z_{e6}	−0.032
	0.073		0.078		0.086
	Tool (mm)				
x_{eT}	−28.853	y_{eT}	41.004	z_{eT}	59.913
	0.079		0.074		0.075

parameters and the coordinates of each ball centre are the same as those used in simulation **III**. The initial values of the coordinate transformation are the same as those used in simulation **II**. The *a priori* standard deviation is given from the radius of each ball and the *a priori* error estimation. In this case, the radius of the ball is 5 mm and the positioning accuracy before calibration is 0.1 mm, and thus it approximates 0.01 radian.
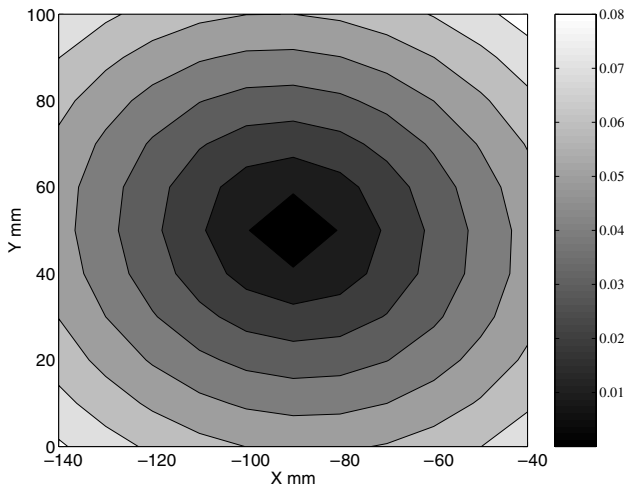
Figure 7. Positioning accuracy of the parallel mechanism after simulation **III** estimated from the law of error propagation.

Table 4. Results of simulation **IV**: identified values (upper) and standard deviations (lower).

	Base plate (mm)				
x_{b1}	0 (nominal)	y_{b1}	0 (nominal)	z_{b1}	0 (nominal)
	0 (nominal)		0 (nominal)		0 (nominal)
x_{b2}	0 (nominal)	y_{b2}	17.405	z_{b2}	0 (nominal)
	0 (nominal)		0.072		0 (nominal)
x_{b3}	−141.826	y_{b3}	99.310	z_{b3}	0 (nominal)
	0.064		0.074		0 (nominal)
x_{b4}	−156.902	y_{b4}	90.592	z_{b4}	−0.107
	0.071		0.075		0.085
x_{b5}	−156.904	y_{b5}	−73.167	z_{b5}	−0.058
	0.072		0.074		0.084
x_{b6}	−141.863	y_{b6}	−81.929	z_{b6}	−0.031
	0.065		0.070		0.082
	Linear actuator (mm)				
l_1	235.033	l_2	235.023	l_3	235.037
	0.068		0.063		0.066
l_4	234.983	l_5	234.997	l_6	235.104
	0.079		0.078		0.078
	End plate (mm)				
x_{e1}	0 (nominal)	y_{e1}	0 (nominal)	z_{e1}	0 (nominal)
	0 (nominal)		0 (nominal)		0 (nominal)
x_{e2}	0 (nominal)	y_{e2}	81.927	z_{e2}	0 (nominal)
	0 (nominal)		0.075		0 (nominal)
x_{e3}	−7.617	y_{e3}	86.288	z_{e3}	0 (nominal)
	0.065		0.076		0 (nominal)
x_{e4}	−78.521	y_{e4}	45.373	z_{e4}	0.042
	0.071		0.074		0.084
x_{e5}	−78.522	y_{e5}	36.520	z_{e5}	0.106
	0.070		0.074		0.084
x_{e6}	−7.527	y_{e6}	−4.357	z_{e6}	0.043
	0.065		0.072		0.081
	Tool (mm)				
x_{eT}	−28.887	y_{eT}	41.034	z_{eT}	59.994
	0.076		0.070		0.069

Figure 8. Residual norm at each step in simulations **III** and **IV**.
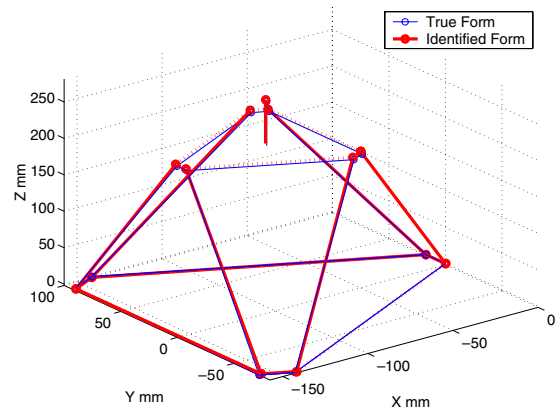
Figure 9. Identified form of the parallel mechanism (simulation **VI**).

Figure 10. Positioning accuracy of the parallel mechanism after simulation **VI** estimated from the law of error propagation.

In simulation **IV**, all kinematic parameters, each ball centre, and coordinate transformation parameters are identified without divergence. The residual norms of the observation equation vector $|O|$ transits are shown in figure 8.

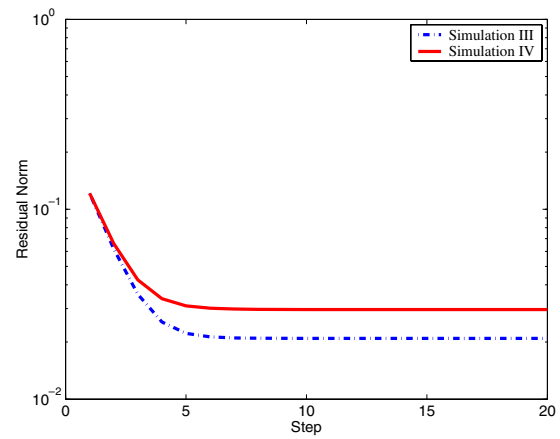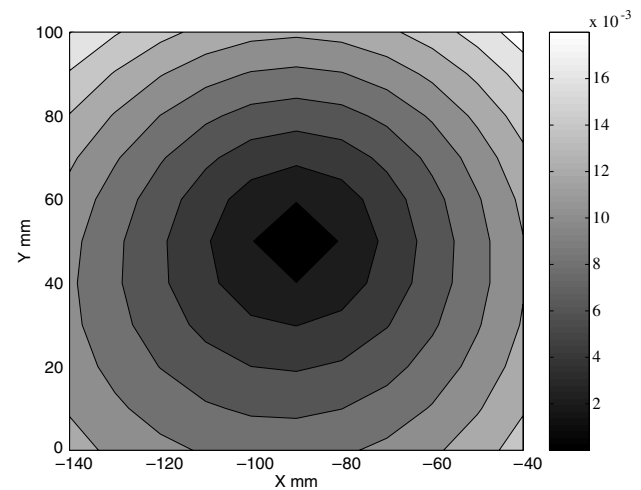Identified values and standard deviations appear in table 4. The overview of the identified calibration system is shown in figure 9. Positioning accuracy after simulation **IV** is estimated as well as it was in simulation **III**. Figure 10 shows the standard deviation of positioning accuracy on the horizontal plane $Z = 400$ mm. Positioning accuracy improved from 0.1 mm to 10 μm through simulation **IV**.

4. Discussion

In this section, we discuss

(i) the effect of *a priori* knowledge and
(ii) the effect of improving the observation equation,

by comparing the results of the simulations.

4.1. Effect of a priori knowledge

Comparing simulations **I** and **II** with simulations **III** and **IV**, we see that the calibration calculation becomes robust with *a priori* knowledge. That is because *a priori* knowledge eliminates the correlation between the parameters and anchors the identified values.

When the correlations are strong, the generalized inverse matrix written in equation (5) becomes singular. Thus, the updating vector becomes very large and each kinematic parameter value diverges. On the other hand, using *a priori* knowledge weakens these correlations because the submatrix of the Jacobian matrix written in equation (7) is the unit matrix. Use of the Jacobian matrix including the unit matrix means that some kinematic parameters are directly measured independently of the others. This independence of measurement eliminates correlation and improves the singularity of the Jacobian matrix.

After these correlations are eliminated, the update vector may be very large when the pose of the tool is close to its singular position. In such a case, *a priori* knowledge operates as an anchor. This anchoring strength depends on the initial estimation prior to the calibration. Note that when the prior estimation is irrelevant, it obstructs the appropriate parameter identification. When the anticipated standard deviation is very small and the initial value of the parameter is far from its true value, its identified value cannot reach its true value because of too strong anchoring. For example, when the standard deviation of the parameter is pre-estimated at zero, the identified value is not updated from its initial value. Therefore, weak anchoring strength must be assumed when using *a priori* knowledge for calibration. From the viewpoint of the weakness of the anchoring strength, the approximation given from the law of error propagation with initial tolerances is appropriate. For this reason, it is reasonable to use *a priori* knowledge estimated without extra measurement.

4.2. Effect of the improvement of the observation equation

Next, we discuss the difference between the results of the simulations using different observation equations.

Comparing simulation **III** with simulation **IV**, positioning accuracy after simulation **IV** is higher than that after simulation **III**, which means that the calibration in simulation **IV** is more effective than that in simulation **III** (see figures 7 and 10). This difference comes from the difference of observation equations used in each calibration. Using the observation equation given by equation (9), information about the distance between the centre of the ball and the position of the tool is available. On the other hand, using the observation equation given by equation (10), information about the relative coordinates between them is available. This difference influences the

Jacobian matrix. Each element of the Jacobian matrix is the partial differential coefficient of the observation equation. Here we assume that a parameter influences the positioning error but not the value obtained in equation (9). As a result, this parameter cannot be identified from the observation equation given by equation (9). Having done the simulations, we are now certain that the positioning error includes three-dimensional data. In turn, we are certain that at least one element of the observation equation vector written in equation (10) is influenced by the error due to this parameter. This means that using the observation equation (10), we can observe the influence due to any kinematic parameter error when the parameters considered are linearly independent of each other. This fact suggests the superiority of using the transformed coordinates for calibration.

Comparing the condition numbers of the covariance matrix given from equations (9) and (10), we determine that the former is 1.3×10^8 and the latter is 6.9×10^8. This difference means that the observation equation (10) provides better conditions for the calibration [14]. As shown in tables 3 and 4, standard deviations after calibration in simulation **IV** become smaller than those in simulation **III**. This fact also implies the effectiveness of the calibration using the transformed coordinates.

5. Conclusion

We described here a method for *artefact calibration* with *a priori* knowledge. Features of this method include:

- getting *a priori* knowledge without any extra measurements,
- using *a priori* knowledge to eliminate the correlations between kinematic parameters,
- using *a priori* knowledge to anchor the identified values of kinematic parameters and
- using transformed coordinates for the observation equation.

In the simulations, we estimate *a priori* knowledge from the initial values and tolerances of kinematic parameters. Using the law of error propagation, we also estimate other *a priori* knowledge of extra parameters attached to the calibration object without any extra measurement.

Through the simulations, we confirmed that *a priori* knowledge given by our method provides the robustness for the calibration. This robustness comes from the unit matrix included in the Jacobian matrix and the restriction of the updating vector in the Newton–Raphson method.

We note that improper *a priori* knowledge obstructs the appropriate parameter identification. We also note that adequate weak anchoring strength, in other words, reasonable largeness of *a priori* standard deviations of kinematic parameters, must be assumed when using *a priori* knowledge for calibration. We conclude that our method gives appropriate *a priori* knowledge.

Comparing the simulation results, we confirmed the superiority of using the transformed coordinates for the observation equations. This observation equation gives a better condition and simulation results than does using the radii of measured balls. Because the error of kinematic

parameters causes the three-dimensional positioning error of the end-effector, the observation equation of the transformed coordinates cannot fail to detect it.

Through the calibration made on the assumption that the repeatability of positioning is 1 μm and the accuracy of the calibration artefact is 1 μm, the positioning accuracy of the parallel mechanism is improved from 0.1 mm to 10 μm. This value is still lower than its repeatability. More improvement of the positioning accuracy can be expected by changing the arrangement of measuring points in the workspace [4].

References

[1] Everett L, Driels M and Mooring B 1987 Kinematic modelling for robot calibration *Proc. IEEE Int. Conf. Robotics Automat.* p 183

[2] Renders J, Rossignol E, Becquet M and Hanus R 1991 Kinematic calibration and geometrical parameter identification for robots *IEEE Trans. Robot. Autom.* **7** 721

[3] Bennett D and Hollerbach J 1991 Autonomous calibration of single-loop closed kinematic chains formed by manipulators with passive endpoint constraints *IEEE Trans. Robot. Autom.* **7** 597

[4] Sato O, Hiraki M, Takamasu K and Ozono S 2001 Calibration of 2-DOF parallel mechanism *ICPE2001* p 734

[5] Bai S and Yeong Teo M 2003 Kinematic calibration and pose measurement of a medical parallel manipulator by optical position sensors *J. Robot. Syst.* **20** 201

[6] Khosla P 1989 Categorization of parameters in the dynamic robot model *IEEE Trans. Robot. Autom.* **5** 261

[7] Denavit J and Hartenberg R 1995 A kinematic notation for lower-pair mechanisms based on matrices *J. Appl. Mech.* **22** 215

[8] Zhuang H, Roth Z and Hamano F 1992 A complete and parametrically continuous kinematic model for robot manipulators *IEEE Trans. Robot. Autom.* **8** 451

[9] Zhuang H 1997 Self-calibration of parallel mechanisms with a case study on Stewart Platforms *IEEE Trans. Robot. Autom.* **13** 387

[10] Khalil W and Besnard S 1999 Self calibration of Stewart–Gough parallel robots without extra sensors *IEEE Trans. Robot. Autom.* **15** 1116

[11] Nanua P, Waldron K and Murthy V 1990 Direct kinematic solution of a Stewart Platform *IEEE Trans. Robot. Autom.* **6** 438

[12] Wampler C, Hollerbach J and Arai T 1995 An implicit loop method for kinematic calibration and its application to closed-chain mechanisms *IEEE Trans. Robot. Autom.* **11** 710

[13] Furutani R, Shimojima K and Takamasu K 2002 Parameter calibration of articulated CMM *euspen2002* p 605

[14] Shiu Y and Ahmad S 1989 Calibration of wrist-mounted robotic sensors by solving homogeneous transform equations of the form $AX = XB$ *IEEE Trans. Robot. Autom.* **5** 16